

Molecular Structures, Bond Energies, and Bonding Analysis of Group 11 Cyanides TM(CN) and Isocyanides TM(NC) (TM = Cu, Ag, Au)[†]Oliver Dietz,[‡] Víctor M. Rayón,^{*§} and Gernot Frenking^{*§}*Institut für Organische Chemie, J.W. Goethe-Universität Frankfurt, Marie-Curie-Strasse 11, D-60439 Frankfurt (Main), Germany, and Fachbereich Chemie, Philipps-Universität Marburg, Hans-Meerwein-Strasse, D-35032 Marburg, Germany*

Received February 3, 2003

We report on quantum chemical calculations at the DFT (BP86/TZP) and ab initio (CCSD(T)/III+) levels of the title compounds. The geometries, vibrational spectra, heats of formation, and homolytic and heterolytic bond dissociation energies are given. The calculated bond length of Cu–CN is in reasonable agreement with experiment. The theoretical geometries for CuNC and the other group 11 cyanides and isocyanides which have not been measured as isolated species provide a good estimate for the exact values. The theoretical bond dissociation energies and heats of formation should be accurate with an error limit of ± 5 kcal/mol. The calculation of the vibrational spectra shows that the C–N stretching mode of the cyanides, which lies between 2170 and 2180 cm^{-1} , is IR inactive. The $\omega_1(\text{C–N})$ vibrations of the isocyanides are shifted by ~ 100 cm^{-1} to lower wavenumbers. They are predicted to have a very large IR intensity. The nature of the metal–ligand interactions was investigated with the help of an energy partitioning analysis in two different ways using the charged fragments $\text{TM}^+ + \text{CN}^-$ (TM = transition metal) and the neutral fragments $\text{TM}^* + \text{CN}^*$ as bonding partners. The calculations suggest that covalent interactions are the driving force for the formation of the TM–CN and TM–NC bonds, but the finally formed bonds are better described in terms of interactions between TM^+ and CN^- , which have between 73% and 80% electrostatic character. The contribution of the π bonding is rather small. The lower energy of the metal cyanides than that of the isocyanides comes from the stronger electrostatic interaction between the more diffuse electron density at the carbon atom of the cyano ligand and the positively charged nucleus of the metal.

Introduction

The nature of the chemical bond is usually described using qualitative bonding models, which proved to be useful as ordering schemes for the manifold of chemical structures. In transition-metal (TM) chemistry, the analysis of the bonding situation is frequently carried out within the framework of the Dewar–Chatt–Duncanson (DCD) model,¹ according to which the metal–ligand interaction is discussed in terms of metal \leftarrow ligand donation and metal \rightarrow ligand back-donation. The DCD model is based on heuristic considerations, and the analysis of the metal–ligand bond

is often done using charge partitioning schemes.² However, accurate theoretical calculations clearly provide the best basis for the development and support of a chemical model which is in agreement with the physical origin of the chemical bond.³ Two years ago we started a research program with the aim of analyzing the chemical bonding in terms of rigorously defined and physically meaningful contributions to the bond energy. The first summary of the research projects which have been finished up to now has been recently published.⁴ The results demonstrate that the DCD molecular orbital model is beautifully recovered and quantitatively supported. The energy analysis also makes it

* Authors to whom correspondence should be addressed. E-mail: frenking@chemie.uni-marburg.de (G.F.); vmr@chemie.uni-marburg.de (V.M.R.).

[†] Theoretical Studies of Inorganic Compounds. 30. Part 29: Esterhuysen, C.; Frenking, G. *Chem.–Eur. J.*, in press.

[‡] J.W. Goethe-Universität Frankfurt.

[§] Philipps-Universität Marburg.

(1) (a) Dewar, M. J. S. *Bull. Soc. Chim. Fr.* **1951**, 18, C79. (b) Chatt, J.; Duncanson, L. A. *J. Chem. Soc.* **1953**, 2929.

(2) Recent reviews: (a) Frenking, G.; Fröhlich, N. *Chem. Rev.* **2000**, 100, 717. (b) Frenking, G. *J. Organomet. Chem.* **2001**, 635, 9. (c) Frenking, G. In *Modern Coordination Chemistry: The Legacy of Joseph Chatt*; Leigh, G. J., Winterton, N., Eds.; The Royal Society: London, 2002; p 111.

(3) Kutzelnigg, W. In *Theoretical Models of Chemical Bonding*; Maksic, Z. B., Ed.; Springer-Verlag: Berlin, 1990; Vol. 2, p 1.

(4) Frenking, G.; Wichmann, K.; Fröhlich, N.; Loschen, C.; Lein, M.; Frunzke, J.; Rayón, V. M. *Coord. Chem. Rev.* **2003**, 238–239, 55.

possible to estimate the relative strength of the electrostatic and covalent contributions to the interatomic attraction.

As a further extension of this project, we report here the results of an analysis of the bonding situation in the monomeric transition-metal (I) cyanides TM(CN) and isocyanides TM(NC) (TM = Cu, Ag, Au). The nature of the Cu–CN bond is not yet firmly established, and to the best of our knowledge, there are no theoretical studies on the Ag–CN and Au–CN metal–ligand interactions. It will also be interesting to address the question of the preferred equilibrium structure taking into account the variety of them observed up to now in monomeric single-metal cyanides (linear cyanides X–CN, linear isocyanides X–NC, and T-shape bridged structures). The aim of this work is to provide insight into the bonding situation in the title compounds by means of a decomposition analysis of the bond energy. The partitioning scheme we have chosen is the EPA (energy partitioning analysis) method, which is based on ideas suggested by Morokuma⁵ and Ziegler and Rauk.⁶ An important feature of this method has already been pointed out in the previous paragraph, that is, the quantification of the molecular orbital interactions which are heuristically proposed in the DCD model. We stress that the EPA allows us to go beyond the DCD model, also giving information about the relative strength of the electrostatic and orbital interactions and the role of the Pauli repulsion.

We will comment shortly on two more reasons why we believe that a decomposition analysis of the bond energy is advisable for the study of the bonding situation in the title compounds. The DCD model assumes a *donor–acceptor* interaction between a closed-shell donor and a closed-shell acceptor although the bonding situation in many transition-metal compounds is perhaps better described as an electron-sharing interaction between two fragments, where each fragment provides one electron to a single bond. We will refer to the two types of interaction as the *heterolytic approach* and the *homolytic approach*, respectively. The EPA method makes it possible to study the metal–ligand bond from both points of views.⁷ This will allow us to address the question of which one is the best picture to discuss the bonding situation in the TM(CN) and TM(NC) (TM = Cu, Ag, Au) compounds.

Previous theoretical studies on the bonding situation in Cu–CN^{8–10} focus on the analysis of the wave function and/or the charge distribution. We recall that the decomposition analysis of the interaction energy gives a *direct* answer to the question about the strength of the covalent and electrostatic bonding. We remind the reader that a discussion in terms of electrostatic and covalent bonding based only on the distribution of the electron density can be misleading.

In particular the information given by atomic charges must be used with caution because the electron density distribution of an atom in a molecule is usually very anisotropic. An atom which carries an overall positive charge may have a local area of negative charge concentration, which can lead to strong electrostatic attraction with another positively charged atom. Consideration of atomic partial charges would in such cases deceptively predict charge repulsion. On the other hand, we must also keep in mind that the charge distribution in a molecule strongly influences the energy levels of the interacting orbitals, and thus, it indirectly influences the covalent interactions. For these reasons, a partitioning of the interaction energy is clearly advisable when the chemical bond is analyzed in terms of covalent and electrostatic contributions. To the best of our knowledge, this is the first decomposition analysis of the bond energy of the title compounds.

Besides the analysis of the bonding situation we also report the theoretically predicted geometries, rotational constants, vibrational spectra, bond dissociation energies, and heats of formation of TM(CN) and TM(NC). Recently, the precise molecular structure of monomeric copper cyanide in the gas phase has been published by Ziurys et al.¹¹ The latter work was the first accurate characterization of a transition-metal cyanide. The product of the gas-phase reaction between copper vapor and cyanogen (NCCN) was analyzed by millimeter/submillimeter-wave spectroscopy. From the observed spectra, it was possible to unambiguously conclude that the reaction product is linear with copper bonded to the carbon atom, not to nitrogen. Copper isocyanides, if present, must be a very minor component of the reaction. The study allows a direct comparison with data obtained from theoretical calculations. Experimental studies of silver and gold cyanides, on the other hand, are scarce, and only limited data are available.

Computational Details

The geometry optimizations, frequency calculations, and bonding analysis were performed at the nonlocal DFT level of theory using the exchange functional of Becke¹² and the correlation functional of Perdew¹³ (BP86). Relativistic effects have been considered by means of the zero-order regular approximation (ZORA).^{14,15} Uncontracted Slater-type orbitals (STOs) were employed as basis functions for the SCF calculations.¹⁶ All the basis sets used have triple- ζ quality augmented by one set of d and f polarization functions on C and N and one set of f-type functions on Cu, Ag, and Au. The $(n-2)s^2$, $(n-2)p^6$, and $(n-1)d^{10}$ core electrons of the metal atoms were treated by the frozen-core approximation.¹⁷ This level of theory is denoted as BP86/TZP. An auxiliary set of s, p, d, f, and g STOs was used to fit the molecular densities and to represent the Coulomb and exchange potentials accurately in

(5) Morokuma, K. *J. Chem. Phys.* **1971**, *55*, 1236.
 (6) Ziegler, T.; Rauk, A. *Theor. Chim. Acta* **1977**, *46*, 1.
 (7) The bonding situation in a polar bond with the EPA method using the homolytic and heterolytic approaches has previously been reported for CH₃Li: Bickelhaupt, F. M.; van Eikema Hommes, N. J. R.; Guerra, C. F.; Baerends, E. J. *Organometallics* **1996**, *15*, 2923.
 (8) Nelin, C. J.; Bagus, P. S.; Philpott, M. R. *J. Chem. Phys.* **1987**, *87*, 2170.
 (9) Bauschlicher, C. W., Jr. *Surf. Sci.* **1985**, *154*, 70.
 (10) Boldyrev, A. I.; Li, X.; Wang, L. *J. Chem. Phys.* **2000**, *112*, 3627.

(11) Grotjahn, D. B.; Brewster, M. A.; Ziurys, L. M. *J. Am. Chem. Soc.* **2002**, *124*, 5895.
 (12) Becke, A. D. *Phys. Rev. A* **1988**, *38*, 3098.
 (13) Perdew, J. P. *Phys. Rev. B* **1986**, *33*, 8822.
 (14) Snijders, J. G. *Mol. Phys.* **1978**, *36*, 1789.
 (15) Snijders, J. G.; Ros, P. *Mol. Phys.* **1979**, *38*, 1909.
 (16) Snijders, J. G.; Baerends, E. J.; Vernooijs, P. *At. Nucl. Data Tables* **1982**, *26*, 483.
 (17) Baerends, E. J.; Ellis, D. E.; Ros, P. *Chem. Phys.* **1973**, *2*, 41.

Table 1. Calculated Bond Distances r , Rotational Constants B , Bond Dissociation Energies D_e and D_0 , and Enthalpies of Formation ΔH_f° of the Complexes TM(CN) and TM(NC) (TM = Cu, Ag, Au) at the BP86/TZP Level of Theory

	$r[\text{TM}-\text{CN}]$ (Å)	$r[\text{C}-\text{N}]$ (Å)	B (MHz)	E_{rel} (kcal/mol)	$D_e(\text{homolytic})$ (kcal/mol)	$D_0(\text{homolytic})$ (kcal/mol)	$D_e(\text{heterolytic})^b$ (kcal/mol)	$D_0(\text{heterolytic})^b$ (kcal/mol)	ΔH_f° ^c (kcal/mol)
CuCN	1.778 1.82962(4)^a	1.168 1.16213(3)^a	4379.72	0.0	98.0	96.4	215.5 (186.9)	213.8 (185.3)	87.7
CuNC	1.749	1.182	4773.08	14.3	97.7	96.1	173.7 (186.6)	172.0 (185.0)	88.0
AgCN	2.014	1.167	3263.93	10.0	83.7	82.5	201.2 (172.6)	199.9 (171.4)	101.8
AgNC	2.016	1.181	3456.35	15.3	87.7	86.5	163.6 (176.5)	162.3 (175.4)	97.8
AuCN	1.920	1.168	3196.95	0.0	83.2	81.9	186.4 (168.9)	185.0 (167.6)	89.4
AuNC	1.939	1.183	3348.21	25.2	85.2	83.9	161.5 (171.0)	160.1 (169.6)	87.4
				27.3	67.9	67.0	171.1 (153.6)	170.1 (152.7)	104.5
					72.7	71.8	149.1 (158.6)	148.1 (157.5)	99.7
					90.0	88.4	229.9 (213.5)	228.2 (211.9)	101.8
					93.7	92.1	210.0 (217.4)	208.3 (215.6)	98.1
					64.8	63.7	204.7 (188.3)	203.5 (187.2)	126.7
					66.4	65.3	182.6 (190.0)	181.4 (188.8)	125.1

^a Reference 11. ^b The values in parentheses are corrected by the errors of the calculated ionization potentials and electron affinities. ^c Calculated using the theoretically predicted D_0 values and the experimental ΔH_f° values of CN (104.0 kcal/mol) and TM (Cu, 80.9 kcal/mol; Ag, 68.0 kcal/mol; Au, 87.0 kcal/mol) taken from ref 48.

each SCF cycle.¹⁸ The calculations were carried out with the program package ADF(2000.02).^{19,20}

To improve the calculated dissociation energies, CCSD(T)^{21,22} single-point calculations have been carried out with our standard basis set III+²³ using the program package Gaussian 98.²⁴ Basis set III+ comprises small-core effective core potentials²⁵ for the transition metals which are nonrelativistic for Cu and quasi-relativistic for Ag and Au with (441/2111/N1/1) valence basis sets ($N = 4$ for Cu, 3 for Ag, and 2 for Au) and 6-31G(d) all-electron basis sets for the other atoms.²⁶ The exponents of the f-type polarization functions for TM have been taken from the literature.²⁷ The BP86/TZP geometries have been used for the CCSD(T)/ III+ calculations.

- (18) Krijn, J.; Baerends, E. J. *Fit Functions in the HFS-Method* (in Dutch); Internal Report; Vrije Universiteit Amsterdam: Amsterdam, 1984.
- (19) Bickelhaupt, F. M.; Baerends, E. J. *Rev. Comput. Chem.* **2000**, *15*, 1.
- (20) te Velde, G.; Bickelhaupt, F. M.; Baerends, E. J.; van Gisbergen, S. J. A.; Fonseca Guerra, C.; Snijders, J. G.; Ziegler, T. *J. Comput. Chem.* **2001**, *22*, 931.
- (21) Bartlett, R. J.; Stanton, J. F. *Reviews in Computational Chemistry*; VCH: New York, 1994; Vol. 5, p 65.
- (22) (a) Cizek, J. *J. Chem. Phys.* **1966**, *45*, 4256. (b) Pople, J. A.; Raghavachari, K.; Schlegel, H. B.; Binkley, J. S. *Int. J. Quantum Chem.* **1978**, *14*, 545. (c) Bartlett, R. J.; Purvis, G. D. *Int. J. Quantum Chem.* **1978**, *14*, 561. (d) Purvis, G. D.; Bartlett, R. J. *J. Chem. Phys.* **1982**, *76*, 1910. (e) Raghavachari, K.; Trucks, G. W.; Pople, J. A.; Head-Gordon, M. *Chem. Phys. Lett.* **1989**, *157*, 479. (f) Bartlett, R. J.; Watts, J. D.; Kucharski, S. A.; Noga, J. *Chem. Phys. Lett.* **1990**, *165*, 513. Hampel, C.; Peterson, K.; Werner, H.-J. *Chem. Phys. Lett.* **1992**, *190*, 1. (g) Watts, J. D.; Gauss, J.; Bartlett, R. J. *J. Chem. Phys.* **1993**, *98*, 8718.
- (23) Frenking, G.; Antes, I.; Böhme, M.; Dapprich, S.; Ehlers, A. W.; Jonas, V.; Neuhaus, A.; Otto, M.; Stegmann, R.; Veldkamp, A.; Vyboishchikov, S. F. In *Reviews in Computational Chemistry*; Lipkowitz, K. B., Boyd, D. B., Eds.; VCH: New York, 1966; Vol. 8, pp 63–144.
- (24) Frisch, M. J.; Trucks, G. W.; Schlegel, H. B.; Scuseria, G. E.; Robb, M. A.; Cheeseman, J. R.; Zakrzewski, V. G.; Montgomery, J. A., Jr.; Stratmann, R. E.; Burant, J. C.; Dapprich, S.; Millam, J. M.; Daniels, A. D.; Kudin, K. N.; Strain, M. C.; Farkas, O.; Tomasi, J.; Barone, V.; Cossi, M.; Cammi, R.; Mennucci, B.; Pomelli, C.; Adamo, C.; Clifford, S.; Ochterski, J.; Petersson, G. A.; Ayala, P. Y.; Cui, Q.; Morokuma, K.; Malick, D. K.; Rabuck, A. D.; Raghavachari, K.; Foresman, J. B.; Cioslowski, J.; Ortiz, J. V.; Baboul, A. G.; Stefanov, B. B.; Liu, G.; Liashenko, A.; Piskorz, P.; Komaromi, I.; Gomperts, R.; Martin, R. L.; Fox, D. J.; Keith, T.; Al-Laham, M. A.; Peng, C. Y.; Nanayakkara, A.; Gonzalez, C.; Challacombe, M.; Gill, P. M. W.; Johnson, B.; Chen, W.; Wong, M. W.; Andres, J. L.; Gonzalez, C.; Head-Gordon, M.; Replogle, E. S.; Pople, J. A. *Gaussian 98*, revision A.7; Gaussian, Inc.: Pittsburgh, PA, 1998.
- (25) Hay, P. J.; Wadt, W. R. *J. Chem. Phys.* **1985**, *82*, 299.
- (26) (a) Ditchfield, R.; Hehre, W. J.; Pople, J. A. *J. Chem. Phys.* **1971**, *54*, 724. (b) Hehre, W. J.; Ditchfield, R.; Pople, J. A. *J. Chem. Phys.* **1972**, *56*, 2257.

The bonding situation in the TM(CN) complexes was investigated by means of an EPA based on the methods by Morokuma⁵ and Ziegler and Rauk.⁶ Within this method, the (instantaneous) interaction energy between two fragments, ΔE_{int} , is split up into three physically meaningful components:

$$\Delta E_{\text{int}} = \Delta E_{\text{elstat}} + \Delta E_{\text{Pauli}} + \Delta E_{\text{orb}} \quad (1)$$

ΔE_{elstat} gives the electrostatic interaction energy between the fragments, which is calculated with a frozen electron density distribution in the geometry of the complex. ΔE_{Pauli} gives the repulsive four-electron interactions between occupied orbitals. This term is calculated by enforcing the Kohn–Sham determinant of the complex, which results from superimposing its constituent fragments, to be orthonormal through antisymmetrization and renormalization. Finally, ΔE_{orb} gives the stabilizing orbital interaction due to the relaxation of the Kohn–Sham orbitals in the SCF procedure.

The latter term can be further partitioned into contributions by the orbitals which belong to different irreducible representations of the interacting system. The bond dissociation energy (BDE) D_e can be computed summing the fragment preparation energy, ΔE_{prep} , and the interaction energy, ΔE_{int} :

$$-D_e = \Delta E_{\text{prep}} + \Delta E_{\text{int}} \quad (2)$$

where ΔE_{prep} is the energy required to promote the fragments from their equilibrium geometry and electronic ground state to the geometry and electronic state which they have in the complex. Further information and technical details about the EPA method can be found in the literature.^{19,20}

The topological analysis of the electron density distribution has been carried out by means of the AIM-PAC program package.²⁸ The densities have been generated at the BP86/III+ level of theory.

Geometries, Energies, Rotational Constants, and Vibrational Spectra

Table 1 gives the bond lengths, rotational constants, and energies of the six complexes TM(CN) and TM(NC) (TM = Cu, Ag, Au). The harmonic vibrational spectral data for these compounds are shown in Table 2.

- (27) Ehlers, A. W.; Böhme, M.; Dapprich, S.; Gobbi, A.; Höllwarth, A.; Jonas, V.; Köhler, K. F.; Stegmann, R.; Veldkamp, A.; Frenking, G. *Chem. Phys. Lett.* **1993**, *208*, 111.
- (28) AIM-PAC; McMaster University: Hamilton, Ontario, Canada, 1995.

Table 2. Theoretically Predicted and Experimentally Observed Vibrational Spectral Data of the Complexes TM(CN) and TM(NC) (TM = Cu, Ag, Au) at the BP86/TZP Level of Theory^a

	$\omega_1(\sigma)$ (cm ⁻¹)	IR (km mol ⁻¹)	$\omega_2(\sigma)$ (cm ⁻¹)	IR (km mol ⁻¹)	$\omega_3(\pi)$ (cm ⁻¹)	IR (km mol ⁻¹)
CuCN	2177	<0.1	512 480(30) ^b	4.4	255	3.0
CuNC	2080	83.7	535	4.6	161	3.8
AgCN	2171	0.5	397 390(20) ^b	7.2	224	2.2
AgNC	2075	73.6	398	7.4	133	2.0
AuCN	2176	0.4	475	0.3	292	0.6
AuNC	2065	63.2	445	0.2	190	2.5

^a The calculated wavenumbers of the harmonic vibrations are unscaled.^b Reference 10.

The calculated bond lengths and the rotational constant of CuCN are in reasonable agreement with the results of the spectroscopic study by Ziurys et al.¹¹ The theoretical Cu–CN distance is slightly shorter (1.778 Å) than the very precise experimental value (1.82962(4) Å), while the calculated and observed C–N distances agree very well. It is remarkable that the BP86/TZP value for the Cu–CN bond length is shorter than the experimental value because all previous theoretical studies using *ab initio*^{8–10} or DFT (B3LYP)¹⁰ methods gave values which are too long (1.853–1.98 Å) except for an MP2 calculation which gives a fortuitously accurate value of 1.826 Å.¹⁰

Experimental geometries for CuNC and monomeric silver and gold cyanides and isocyanides are not available. The calculated values shall be compared with the results of neutral diffraction measurements of solid AgCN, AgNC, AuCN, and AuNC. A recent study by Hibble et al.²⁹ indicates that the Ag–CN and Ag–NC bonds have the same length (2.16 Å), which is in agreement with our calculations, which predict that the Ag–CN distance (2.014 Å) is very similar to the Ag–NC bond length (2.016 Å). The differences between the calculated and experimental metal–ligand distances may partly be caused by the intermolecular interactions in the solid state. Metal cyanides exhibit complex structures, and the metal atoms are usually bonded to more than one ligand.^{29–32} Considerably different bond lengths for Ag–CN and Ag–NC have been reported in another neutron diffraction study by Bowmaker et al.³¹ (Ag–C = 2.15(6) Å, Ag–N = 1.86(8) Å), but the accuracy of these values has been put into doubt.²⁹ For gold cyanide and isocyanide the computed bond lengths are also rather similar (Au–C = 1.920 Å, Au–N = 1.939 Å), which is at variance with the values reported by Bowmaker et al. for solid AuCN showing very different metal–ligand distances (Au–C = 2.06(2) Å, Au–N = 1.82(2) Å).³¹ We suggest a reevaluation of the structure of AuCN and AuNC in the solid state as was done by Hibble et al.²⁹ for the silver compounds.

The calculations indicate that the trend, of the metal–ligand distances follow the orders Cu–CN < Au–CN <

Ag–CN and Cu–NC < Au–NC < Ag–NC. The shorter bond of the gold compounds compared with the silver species is caused by relativistic effects which are particularly strong for Au.³³ The calculations predict that the isocyno compounds always have longer C–N bond lengths (1.181–1.183 Å) than the cyano compounds (1.167–1.168 Å). It will be difficult to measure the difference experimentally, but the C–N stretching frequency should make it possible to verify the theoretical prediction. Table 2 shows that the C–N stretching mode of the isocyanides is ~100 cm⁻¹ lower lying than in the cyanides. We suggest a combined IR/Raman investigation of the cyanides and isocyanides because the C–N stretching mode of the cyanides has a very low IR intensity while the IR signals of the isocyanides should be rather strong.⁴⁹ For the cyanides, only the IR frequencies of the Cu–CN and Ag–CN stretching modes have been reported.¹⁰ The calculated values are in excellent agreement with experiment (Table 2).

Table 1 also lists the relative energies of the cyanides and isocyanides, the metal–ligand BDEs for homolytic and heterolytic bond breaking, and the heats of formation of the six complexes. To the best of our knowledge, no experimental data of these quantities have been reported for the monomeric species except for an estimate of the energy difference between CuCN and CuNC, which was published in the spectroscopic study of Ziurys et al.¹¹ The authors report a lower limit of 5 kcal/mol for the energy difference between CuCN and the energetically higher lying CuNC. Our calculated values of 10.0 kcal/mol (CCSD(T)/III+) and 14.3 kcal/mol (BP86/TZP) are in agreement with the experimental estimate. Previous theoretical studies of copper cyanide and isocyanide give similar values as reported here.^{10,34} The calculations predict that the silver compounds exhibit a similar energy difference between the cyanide and isocyanide while AuCN is significantly (27.3 kcal/mol at CCSD(T)/III+ and 25.2 kcal/mol at BP86/TZP) more stable than AuNC.

The theoretically predicted bond dissociations energies of the homolytic bond breaking at CCSD(T)/III+ and BP86/TZP are very similar (Table 1). This is gratifying, and we think that the calculated values should be quite accurate. The theoretical values suggest that the bond strength of the cyanides has the order Cu–CN > Au–CN > Ag–CN while the isocyanides exhibit the trend Cu–NC > Ag–NC > Au–NC.³⁶ The calculated D_0 values for the reactions TM(CN) → TM + CN and TM(NC) → TM + CN have been used to calculate heats of formation of the cyanides and isocyanides. Table 1 shows that the compounds have strongly positive values of $\Delta H_f(298\text{ K})$.

(33) Pyykkö, P. *Chem. Rev.* **1988**, 88, 563.(34) García Cuesta, I.; Sánchez de Merás, A. Nebot Gil, I. *Chem. Phys.* **1993**, 170, 1.(35) Bouslama, L.; Daoudi, A.; Mestdagh, H.; Rolando, C.; Suard, M. *J. Mol. Struct.: THEOCHEM* **1995**, 330, 187.

(36) The trend of the bond energies is strongly influenced by relativistic effects. We carried out BP86/TZP calculations without relativistic corrections, which gave BDEs showing the trend Cu–CN > Ag–CN > Au–CN. We do not report further details because in this work we focus on the results which come from relativistic calculations.

(37) Bradforth, S. E.; Kim, E. H.; Arnold, D. W.; Neumark, D. M. *J. Chem. Phys.* **1993**, 98, 800.(29) Hibble, S. J.; Cheyne, S. M.; Hannon, A. C.; Eversfield, S. G. *Inorg. Chem.* **2002**, 41, 1042.(30) Bryce, D. L.; Wasylishen, R. E. *Inorg. Chem.* **2002**, 41, 4131.(31) Bowmaker, G. A.; Kennedy, B. J.; Reid, J. C. *Inorg. Chem.* **1998**, 37, 3968.(32) Sharpe, A. G. *The Chemistry of the Cyano Complexes of the Transition Metals*; Academic Press: London, 1976.

Table 3. Ionization Potentials for Cu, Ag, and Au and Adiabatic Electron Affinity of CN at the CCSD(T)/III+ and BP86/TZP Levels of Theory^a

	CCSD(T)/III+	dev	BP86/TZP	dev	exptl ^b
Ionization Energies					
Cu	6.93	-0.79	8.71	+0.99	7.73
Ag	6.94	-0.64	8.09	+0.51	7.58
Au	8.67	-0.55	9.68	+0.46	9.23
Electron Affinities					
CN	3.63	-0.23	3.61	-0.25	3.86

^a All values in electronvolts. ^b The experimental values of the ionization potentials have been taken from ref 48, while the electron affinities are from ref 37.

Table 1 shows that the BDEs of the heterolytic processes $\text{TM}(\text{CN}) \rightarrow \text{TM}^+ + \text{CN}^-$ and $\text{TM}(\text{NC}) \rightarrow \text{TM}^+ + \text{CN}^-$ are as expected higher than the values for the homolytic reactions. There is a significant difference between the values predicted at CCSD(T)/III+ and BP86/TZP for the former reactions. The DFT calculations give clearly lower bond energies for the heterolytic bond breaking than CCSDT/III+. The origin of this difference can be traced back to the calculation of the metal cation TM^+ . Table 3 shows the experimental and calculated ionization potentials of the metals and the (adiabatic) electron affinity of the cyanide radical. It can be seen that the ionization potentials are underestimated at the CCSD(T)/III+ level of theory (by 0.55–0.79 eV) whereas they are overestimated at BP86/TZP (by 0.46–0.99 eV). Both methods calculate the electron affinity of CN slightly too low. We corrected the directly calculated BDEs yielding $\text{TM}^+ + \text{CN}^-$ by adding the deviation between the calculated and experimental ionization energies of TM and electron affinity of CN. The corrected values at CCSD(T)/III+ and BP86/TZP agree very nicely with each other (Table 1). Therefore, we think that the latter values are quite reliable.

A previous theoretical calculation at the multireference-CI level of the BDE of homolytic bond breaking of Cu–CN by Garcia Cuesta et al.³⁴ gave $D_e = 100.8$ kcal/mol, which is similar to our CCSD(T)/III+ value of 98.0 kcal/mol. Surprisingly, a very recent theoretical study at the CCSD(T)/6-311+G(3d)//CCSD(T)/6-311+G(d) level by Boldyrev et al.¹⁰ calculated a much higher value, $D_e = 120.4$ kcal/mol. We recalculated the bond energy of CuCN at CCSD(T)/6-311+G(3d)//BP86/TZP and found $D_e = 97.7$ kcal/mol. We think that there is an error in the theoretical value of Boldyrev et al.¹⁰ The calculated values of Garcia Cuesta et al.³⁴ and our data suggest that the true BDE of CuCN is $D_e = 100 \pm 5$ kcal/mol. An error estimate of ± 5 kcal/mol also seems reasonable for the other BDE values given in Table 1.

There is only one previous paper which reports calculated BDEs of heterolytic bond breaking of $\text{TM}(\text{CN})$ and $\text{TM}(\text{NC})$. Veldkamp and Frenking³⁸ calculated at the QCISD(T)/II level the bond energies of Ag–CN and Au–CN, yielding closed-shell ions. Basis set II has 6-31G(d) all-electron basis sets for C and N and the following contractions of the Hay–Wadt ECP valence basis set: [3311/2111/211/

1] for Ag and [3311/2111/111/1] for Au.²³ The theoretical values for AgCN (179.3 kcal/mol) and AuCN (228.5 kcal/mol) are 8–10 kcal/mol higher than the CCSD(T)/III+ values shown in Table 1. The difference is mainly caused by the smaller 6-31G(d) basis set for C and N, which was used in the earlier study by Veldkamp and Frenking. Recalculations at the QCISD(T) level using larger basis sets for the main group atoms gave similar values for the heterolytic BDEs of AgCN and AuCN as shown in Table 1.

Analysis of the TM–CN and TM–NC Bonding Situation

Chemical bonds between a transition metal and a ligand are usually discussed in terms of metal \leftarrow ligand donation and metal \rightarrow ligand back-donation between closed-shell ligands and a closed-shell metal fragment. Because the DCD model¹ is conceptually simple, it is applied even in cases where the actual bonding fragments are open-shell species. Examples for this are carbyne complexes $[\text{TM}]\text{CR}$ where the bonding is formally discussed in terms of interactions between charged closed-shell fragments $[\text{TM}]^+$ and CR^- instead of between the neutral open-shell species $[\text{TM}]$ and CR , although the latter are the actual dissociation products.³⁹ The CN ligand is also an open-shell species. The metal–ligand bonding in cyano and isocyano complexes is then usually described using $[\text{TM}]^+$ and CN^- as bonding partners. This bonding model is helpful not only for comparing different cyano complexes with each other but also for comparison with isoelectronic carbonyl complexes.

But is the description of the bonding situation using $[\text{TM}]^+$ and CN^- as bonding partners appropriate for a faithful representation of the actual interatomic interactions in cyano and isocyano complexes? To address this question, we carried out EPA calculations of cyanides $\text{TM}(\text{CN})$ and isocyanides $\text{TM}(\text{NC})$ in two different ways. One set of calculations used the charged closed-shell fragments TM^+ and CN^- as bonding partners. In the second approach we took the neutral open-shell (doublet) species $\text{TM} (^2\text{S})$ and $\text{CN} (^2\Sigma^+)$ as interacting fragments. The results not only give an answer to the above question but also provide insight into the nature of the metal–ligand interactions, which can be used for a quantitative description of the bond in terms of covalent versus electrostatic bonding and σ versus π orbital contributions. The results are shown in Table 4.

Before we discuss the numerical results of the EPA calculations, we comment on the atomic partial charges q , which have been calculated at BP86/III+ using the NBO⁴⁰ method and at BP86/TZP using the Hirshfeld partitioning procedure.⁴¹ The data are also shown in Table 4. The values of $q(\text{TM})$ should be useful to address the question of whether the bonding situation in $\text{TM}(\text{CN})$ and $\text{TM}(\text{NC})$ is better described using charged fragments $\text{TM}^+ + \text{CN}^-$ or with the neutral fragments $\text{TM}^\bullet + \text{CN}^\bullet$. The NBO analysis gives positive charges at the metal atom, $q(\text{TM})$, which are $> +0.5$

(39) Vyboishchikov, S. F.; Frenking, G. *Chem.—Eur. J.* **1998**, *4*, 1439.

(40) Reed, A. E.; Curtiss, L. A.; Weinhold, F. *Chem. Rev.* **1988**, *88*, 899.

(41) Hirshfeld, E. L. *Theor. Chim. Acta* **1977**, *44*, 129.

(38) Veldkamp, A.; Frenking, G. *Organometallics* **1993**, *12*, 4613.

Table 4. Energy Partitioning Analysis of the TM(CN) and TM(NC) Complexes (TM = Cu, Ag, Au) at the BP86/TZP Level and Calculated Atomic Partial Charges q Using the Hirshfeld (NBO) Partitioning Technique^a

	CuCN (heterolytic)	CuCN (homolytic)	CuNC (heterolytic)	CuNC (homolytic)
ΔE_{int}	-215.6	-100.1	-201.2	-85.9
ΔE_{Pauli}	161.2	128.9	142.9	152.2
ΔE_{elstat}	-297.2 (78.9%)	-95.7 (41.8%)	-265.2 (77.1%)	-99.3 (41.7%)
ΔE_{orb}	-79.6 (21.1%)	-133.3 (58.2%)	-78.8 (22.9%)	-138.8 (58.3%)
ΔE_{σ}	-55.5 (69.7%)	-117.0 (87.4%)	-51.9 (65.9%)	-121.5 (87.0%)
ΔE_{π}	-24.1 (30.3%)	-16.9 (12.6%)	-26.9 (34.1%)	-18.1 (13.0%)
$q(\text{Cu})$	+0.37 (+0.62)		+0.39 (+0.75)	
$q(\text{C})$	-0.13 (-0.21)		-0.14 (+0.15)	
$q(\text{N})$	-0.24 (-0.41)		-0.25 (-0.90)	

	AgCN (heterolytic)	AgCN (homolytic)	AgNC (heterolytic)	AgNC (homolytic)
ΔE_{int}	-186.7	-85.1	-171.1	-69.9
ΔE_{Pauli}	142.2	102.7	108.2	106.1
ΔE_{elstat}	-262.8 (79.9%)	-75.4 (40.1%)	-220.5 (78.9%)	-67.9 (38.6%)
ΔE_{orb}	-66.1 (20.1%)	-112.4 (59.9%)	-58.9 (21.1%)	-108.0 (61.4%)
ΔE_{σ}	-49.0 (75.2%)	-103.3 (91.6%)	-41.4 (71.3%)	-99.1 (91.5%)
ΔE_{π}	-16.2 (24.8%)	-9.5 (8.4%)	-16.7 (28.7%)	-9.2 (8.5%)
$q(\text{Ag})$	+0.38 (+0.62)		+0.42 (+0.75)	
$q(\text{C})$	-0.13 (-0.20)		-0.16 (+0.15)	
$q(\text{N})$	-0.25 (-0.42)		-0.26 (-0.90)	

	AuCN (heterolytic)	AuCN (homolytic)	AuNC (heterolytic)	AuNC (homolytic)
ΔE_{int}	-230.2	-91.9	-204.7	-66.7
ΔE_{Pauli}	252.6	178.3	188.3	174.1
ΔE_{elstat}	-364.1 (75.4%)	-128.0 (47.4%)	-287.7 (73.2%)	-108.1 (44.9%)
ΔE_{orb}	-118.7 (24.6%)	-142.2 (52.6%)	-105.3 (26.8%)	-132.7 (55.1%)
ΔE_{σ}	-92.2 (78.3%)	-121.9 (85.5%)	-80.4 (77.0%)	-115.7 (86.9%)
ΔE_{π}	-25.5 (21.7%)	-20.6 (14.5%)	-24.0 (23.0%)	-17.5 (13.1%)
$q(\text{Au})$	+0.27 (+0.40)		+0.29 (+0.54)	
$q(\text{C})$	-0.05 (-0.03)		-0.10 (+0.25)	
$q(\text{N})$	-0.22 (-0.37)		-0.19 (-0.79)	

^a All energies in kilocalories per mole.

for all compounds except AuCN. This means that neutral fragments should be used for the latter molecule but charged fragments for the other compounds. The Hirshfeld method gives positive charges for the metal atoms which are always $< +0.5$. Thus, the calculated atomic partial charges are not very helpful for finding which of the two alternatives is better suited to describe the bonding situation in the cyanides and isocyanides. Note that both methods give clearly smaller positive charges for the gold atom in AuCN and AuNC than for the other metals.

The EPA results of CuCN and CuNC using the fragments of the heterolytic ($\text{TM}^+ + \text{CN}^-$) and homolytic ($\text{TM}^\bullet + \text{CN}^\bullet$) bond breaking shall now be discussed in detail. Table 4 shows that the total interaction energy using the charged fragments is much higher ($\Delta E_{\text{int}} = -215.6$ kcal/mol for CuCN, $\Delta E_{\text{int}} = -201.2$ kcal/mol for CuNC) than for the neutral fragments ($\Delta E_{\text{int}} = -100.1$ kcal/mol and $\Delta E_{\text{int}} = -85.9$ kcal/mol). The electrostatic attraction between the charged fragments in both isomers CuCN and CuNC is also much higher ($\Delta E_{\text{elstat}} = -297.2$ kcal/mol and $\Delta E_{\text{elstat}} = -265.2$ kcal/mol) than between the neutral species ($\Delta E_{\text{elstat}} = -95.7$ kcal/mol and $\Delta E_{\text{elstat}} = -99.3$ kcal/mol).

The calculated values of the Pauli repulsion reveal important information about the metal–ligand interactions. For the heterolytic approach, the ΔE_{Pauli} value of CuCN is higher (161.2 kcal/mol) than for the homolytic approach

(128.9 kcal/mol), but the reverse order is found for CuNC. Here, the Pauli repulsion between the charged fragments is smaller (142.9 kcal/mol) than between the neutral fragments (152.2 kcal/mol). Note that the Pauli repulsion between the charged fragments in CuCN is larger than in CuNC although the Cu–CN distance (1.778 Å) is longer than the Cu–NC distance (1.749 Å). The calculated values for ΔE_{Pauli} can be explained with the shape of the σ HOMO of CN^- , which is mainly a carbon lone-pair orbital which, therefore, has a relatively large extension toward the metal atom in CuCN, yielding large Pauli repulsion. The σ HOMO in neutral CN is only singly occupied and less diffuse. Therefore, the Pauli repulsion between the neutral fragments is larger in CuNC than in CuCN because of the shorter metal–ligand bond length of the former compound.

Very important information about the bonding situation in CuCN and CuNC comes from the orbital term ΔE_{orb} . Table 4 shows that the calculated values for the heterolytic approach ($\Delta E_{\text{orb}} = -79.6$ kcal/mol and $\Delta E_{\text{orb}} = -78.8$ kcal/mol) are significantly smaller than for the homolytic approach ($\Delta E_{\text{orb}} = -133.3$ kcal/mol and $\Delta E_{\text{orb}} = -138.8$ kcal/mol). This means that the relaxation of the wave functions of both isomers releases much less energy when the original wave function comes from $\text{Cu}^+ + \text{CN}^-$ rather than from $\text{Cu}^\bullet + \text{CN}^\bullet$. *This is a striking argument in favor of describing the bonding situation of Cu–CN and Cu–NC in terms of interactions between the charged fragments.*⁷ The EPA calculations thus clearly suggest that the data which are obtained from the heterolytic approach should be used to characterize the Cu–CN and Cu–NC bonds. According to the results which are given in Table 4 the metal–ligand bonds are much more electrostatic (78.9% in CuCN and 77.1% in CuNC) than covalent. The π contributions to the ΔE_{orb} term appear relatively large (30.3% in CuCN and even 34.1% in CuNC), which seems to contradict previous theoretical work by Nelin et al.,⁸ who concluded that there is essentially no π back-bonding in CuCN because the population of the $2\pi^*$ orbital of free CN in the complex is negligible. We point out that the percentage contribution of π interactions in CuCN and CuNC refers to a ΔE_{orb} term which contributes only 21.1% and 22.9% of the total attraction. Also, part of the stabilization of the ΔE_{orb} term comes from the energy lowering of the orbitals caused by the electrostatic field of the other fragment. This effect should be quite large for the occupied orbitals of the negatively charged ligand CN^- in the field of Cu^+ . Thus, the EPA results also suggest that π bonding in CuCN and CuNC is not very important.

We emphasize that the EPA results of the homolytic approach also reveal important information. As shown above, the charged fragments $\text{Cu}^+ + \text{CN}^-$ are the best choice to describe the eventually formed chemical bond between the metal and the ligand although the bond breaking yields the neutral species $\text{Cu}^\bullet + \text{CN}^\bullet$ as reaction products. The EPA results of the homolytic approach reveal information about the *changes* which take place along the reaction coordinate of the bond formation reaction. The ΔE_{orb} term is larger when the neutral fragments rather than the charged species are

employed because it includes the effect of moving the unpaired electron from Cu ($2S$) to the cyano ligand. This is the reason the orbital term of the homolytic approach is larger compared with that of the heterolytic approach. The ΔE_{orb} term contributes even more (58.2% in CuCN and 58.3% in CuNC) to the metal–ligand attraction than the ΔE_{elstat} term when $\text{Cu}^{\bullet} + \text{CN}^{\bullet}$ are used as interacting fragments (Table 4). Thus, covalent interactions are the driving force for the formation of the Cu–CN and Cu–NC bonds although the finally formed bonds have more electrostatic than covalent character. A paradoxical behavior of different energy terms has already been found for the kinetic and potential energy contributions to the chemical bond in H_2^+ and H_2 by Ruedenberg.^{3,42,43} The potential energy of the electrons in the molecules is lower than that of the atoms as required by the virial theorem, which states that the potential energy is half the total energy. Nevertheless, the driving force for the binding interactions is the kinetic energy, which becomes lower in the initial state of the bond formation.⁴³

The EPA results of silver cyanide and isocyanide are not very different from those of the copper systems. The heterolytic approach gives much higher electrostatic bonding (79.9% for AgCN and 78.9% for AgNC) than covalent attraction, while in the homolytic approach the ΔE_{orb} term is the larger component (59.1% for AgCN and 61.4% for AgNC). According to both approaches, π bonding in AgCN and AgNC is even less important than in the copper compounds. Slightly different values are calculated for the gold compounds. Note that the differences of the absolute values of ΔE_{orb} between the homolytic and heterolytic approaches for AuCN and AuNC are much less than in the case of the copper and silver compounds (Table 4). This means that the description of the bonding situation in the gold compounds in terms of the neutral fragments $\text{Au}^{\bullet} + \text{CN}^{\bullet}$ becomes more important compared with that of the Cu and Ag species. In other words, covalent bonding between Au and CN is more important than between Cu and CN and between Ag and CN. This result is in agreement with previous findings about the chemical bonds of group 11 elements.^{2a,44} Table 4 shows that the EPA results exhibit a larger contribution of the ΔE_{orb} term to the attractive interactions in AuCN (24.6%) and AuNC (26.8%) compared with the copper and silver compounds when the heterolytic approach is used. The homolytic approach gives lower values for the percentage contributions of the ΔE_{orb} term in AuCN and AuNC. This is another indication that the heterolytic approach should be used to describe the bonding situation in the molecules. The contribution of the π bonding in AuCN and AuNC remains rather small. The increase of the covalent bonding comes only from the σ orbitals.

Why are the isocyanides less stable than the cyanides? The EPA results shown in Table 4 give an explanation which is not obvious without the energy components of the metal–ligand interactions being known. The Pauli repulsion ΔE_{Pauli}

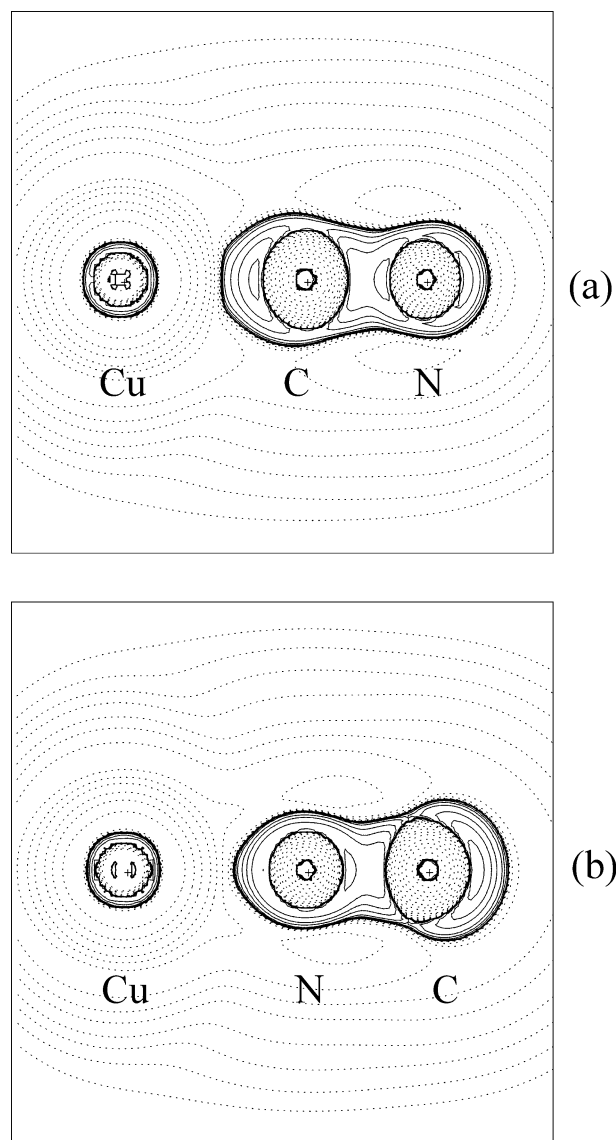


Figure 1. Contour line diagrams of the Laplacian distribution $\nabla^2\rho(\mathbf{r})$ of (a) CuCN and (b) CuNC. Solid lines give areas of charge concentration ($\nabla^2\rho(\mathbf{r}) < 0$), while dashed lines give areas of charge depletion ($\nabla^2\rho(\mathbf{r}) > 0$).

in the isocyanides $\text{TM}(\text{NC})$ is always weaker than in the cyanides $\text{TM}(\text{CN})$. Thus, the latter compounds are lower in energy than the former because the attractive components of the interaction energy ΔE_{int} are larger.⁴⁵ Table 4 shows that it is the electrostatic attraction which is always much larger in $\text{TM}(\text{CN})$ than in $\text{TM}(\text{NC})$. The EPA results suggest that the higher stability of the group 11 cyanides over the isocyanides comes from the stronger charge attraction in the former compounds. This is again a somewhat paradoxical result because the nitrogen atom of CN^- carries a larger negative charge than the less electronegative carbon atom. The calculated partial charges shown in Table 4 indicate that the nitrogen atom in $\text{TM}(\text{CN})$ and $\text{TM}(\text{NC})$ is also more negatively charged than carbon. This is yet another example

(45) This is not a trivial result. Stronger bonds are frequently explained in terms of stronger attraction, but they may also come from less Pauli repulsion. This has recently been found as the reason for the stronger bond of CO compared with N_2 : Esterhuysen, C.; Frenking, G. *Theor. Chem. Acc.* in press.

(42) Ruedenberg, K. *Rev. Mod. Phys.* **1962**, *34*, 326.

(43) Rioux, F. *Chem. Educ.* **2003**, *8*, 1.

(44) Lupinetti, A. J.; Jonas, V.; Thiel, W.; Strauss, S. H.; Frenking, G. *Chem.—Eur. J.* **1999**, *5*, 2573.

showing that the atomic partial charge can be misleading for estimating electrostatic interactions. Nitrogen has more negative charge than carbon, but the *shape* of the electron density distribution is such that more negative charge of the carbon atom is pointing toward the metal and, thus, leads to charge attraction with the metal nucleus. This can be shown visually by comparing the plots of the Laplacian distribution of the electron density $\nabla^2\rho(\mathbf{r})$ of CuCN and CuNC, which are shown in Figure 1. The Laplacian distribution has been found to be a sensitive probe for the topology of the electron density distribution $\rho(\mathbf{r})$.⁴⁶ Solid lines in Figure 1 show areas of electronic charge concentration, while dashed lines give areas of charge depletion. The shape of the Laplacian distribution shows clearly that the carbon atom of the CN ligand has a larger and more diffuse area of charge concentration which points in the direction of the copper atom. The peculiar topology of CN⁻ and isoelectronic CO comes from the σ HOMO orbital, which is also the reason CO has a dipole moment where the negative pole is at the carbon atom.⁴⁷

Summary and Conclusions

The results of this work can be summarized as follows.

The calculated bond length of Cu–CN is in reasonable agreement with experiment. The theoretical geometries for

CuNC and the other group 11 cyanides and isocyanides, which have not been measured as isolated species, are therefore a good estimate for the exact values. The theoretical bond dissociation energies for homolytic and heterolytic bond breaking of the metal–ligand bonds, which are predicted at CCSD(T)/III+ and BP86/TZP, are expected to have an error limit of ± 5 kcal/mol for the calculated bond energies and the theoretically predicted heats of formation. The calculation of the vibrational spectra shows that the C–N stretching mode of the cyanides, which lies between 2170 and 2180 cm^{-1} , is IR inactive. The $\omega_1(\text{C–N})$ vibrations of the isocyanides are shifted by ~ 100 cm^{-1} to lower wavenumbers. They are predicted to have a very large IR intensity.

The analysis of the metal–ligand interactions using the EPA method was carried out using the charged fragments $\text{TM}^+ + \text{CN}^-$ and the neutral fragments $\text{TM}^\bullet + \text{CN}^\bullet$ as bonding partners. The calculations suggest that covalent interactions are the driving force for the formation of the TM–CN and TM–NC bonds, but the finally formed bonds are better described in terms of interactions between TM^+ and CN^- . The metal–ligand bonds have between 73% and 80% electrostatic character. The contribution of the π bonding is rather small. The lower energy of the metal cyanides than that of the isocyanides comes from the stronger electrostatic interaction between the more diffuse electron density at the carbon atom and the positively charged nucleus of the metal.

Acknowledgment. This work was supported by the Deutsche Forschungsgemeinschaft and by the Fonds der Chemischen Industrie. V.M.R. thanks the Secretaría de Estado de Educación y Universidades (MECD-Spain) for support via Grant EX-01-09396368V. We thank Dr. Nikolaus Fröhlich for excellent support of the PC-Cluster “Hückel”. Helpful service by the Hochschulrechenzentrum of the Philipps-Universität Marburg is gratefully acknowledged. Additional computer time was provided by the HHLR Darmstadt.

IC034120U

(46) Bader, R. F. W. *Atoms in Molecules. A Quantum Theory*; Oxford University Press: Oxford, 1990.

(47) Muentzer, J. S. *J. Mol. Spectrosc.* **1975**, *55*, 490.

(48) Lias, S. G.; Bartmess, J. E.; Liebman, J. F.; Holmes, J. L.; Levin, R. D.; Mallard, W. G. *J. Phys. Chem. Ref. Data* **1988**, *17*, Suppl. 1.

(49) The very weak IR intensity of the C–N stretching mode of the cyanides and the rather high IR intensity of the isocyanides indicate that the dipole moment of TM(CN) changes very little during the C–N vibration while the dipole moment of TM(NC) changes much more. We calculated the dipole moments of CuCN and CuNC at the equilibrium geometries at BP86/TZP. We then compared the values with calculated dipole moments using geometries where the C–N distance is stretched or elongated by 0.02 Å. The theoretical dipole moment of CuCN at the optimized geometry (6.25 D) changes very little upon shortening (6.25 D) or elongation (6.26 D), while the dipole moment of CuNC (6.06 D) changes much more when the C–N distance becomes shorter (6.00 D) or longer (6.12 D).